Using Artificial Marks for Semi-Autonomous Wheelchair Localization

Marcel Yañez¹, Mireya García¹, Luis González¹, Alejandro Ramírez²

¹ Instituto Politécnico Nacional-CITEDI, Av. Del Parque No.1310, Tijuana BC, marcel, Igonzal, mgarciav@citedi.mx
² Dpto R&D, PILIMTEC, Châteaugiron,Francia alramirez10@yahoo.fr

Abstract. This paper describes a vision system to detect artificial landmarks for semi-autonomous Wheelchair (SAW) localization in structured indoor environments. The focus is placed on design and implementation of a computer vision based landmark detection system. The artificial landmark has been designed to be a low-cost, easy to implement and any user can be able to printing and placing this type of mark in the environment of its interest. Also, a practical advantage of the method is the computational time saving. It requires less processing resources than traditional methods. Experimental results have shown that the artificial landmark is suited for robot localization and navigation.

Keywords: Artificial landmarks, detection, vision system, wheelchair.

1 Introduction

Recent advances in mobile robotic technologies have already made enormous contributions in many areas. Robots are moving away from factories into environments such as private homes, in order to assist people in daily routines. One of the more researched areas in assistive technology is the development of intelligent or Autonomous Wheelchairs (AWs). By integrating intelligence into a powered wheelchair, a robotic wheelchair has the ability to safely transport a user to their desired destination.

Nevertheless, even though in the last couple of years, numerous research groups around the world have worked in the field of assistive technologies designing and testing Autonomous Wheelchairs [1,2,3,4], there still exists some restrictions in the implementation of these technologies, which affect the performance of AWs and their autonomy.

The restrictions that affect the performance of AWs according to J. Carlos Garcia [5] can be summed up as:

- It's a cost sensitive application, because the economic impact on possible users must be within acceptable terms.
- The system response must be fast, an AW user hopes to move at walking person's speeds.

- The vehicle displacement environment is highly structured.
- The on-board and the surroundings infrastructure cost must be minimum.

And finally, in the case of severely disabled, the security fixes very high limits on the global system reliability.

At present many of the previously mentioned restrictions focus directly on finding the location of the mobile robot, since the effectiveness of the autonomous navigation system of AW is obtained through its reliability and robustness.

In the following sections we will approach a solution for the AW vision system based on the detection of artificial marks placed within the navigation surroundings through a camera mounted on the mobile robot in order to find its own position. Then some of preliminary results using algorithms for finding the location and segmentation marks placed within the surroundings to ease AWs position calculation will be presented.

2 Artificial Mark

The artificial mark used to find the position of the AW is shown in figure 1. It consists fundamentally of 3 elements that altogether produce a precise estimate of the present position of the mobile robot with respect to the position of the mark within the navigation environment map. Each one of these elements can be described according to their function as follows:

- A frame of known dimensions used for discriminating elements of a captured image.
- 2. Four circles of equal diameter and well-known position used for calculating the relative position of the mobile robot.
- 3. One pattern for all the marks that will act as a second discriminator for the false marks that satisfies the first condition (Barker Code).

The integration of these three elements allows us to find the relative position of the robot. Initially with the image captured by the camera mounted on the AW, a scan will be made with the purpose of detecting the first discriminator of a valid mark (the frame of well-known dimensions). This discriminator will allow us to reject those elements that are not part of a valid mark, resulting in a smaller processing time for detecting the valid mark within the image thus reducing the computational cost.

In regard to the election of the format used for the design of the artificial mark, it was designed to be a low-cost, easy to implement and any user can be able to printing and placing this type of mark in the environment of its interest.

3 General Description of the Position System

The block diagram in figure 2 shows the hierarchical organization of the search algorithm. In this diagram, it is included the elements that allow the vision system to

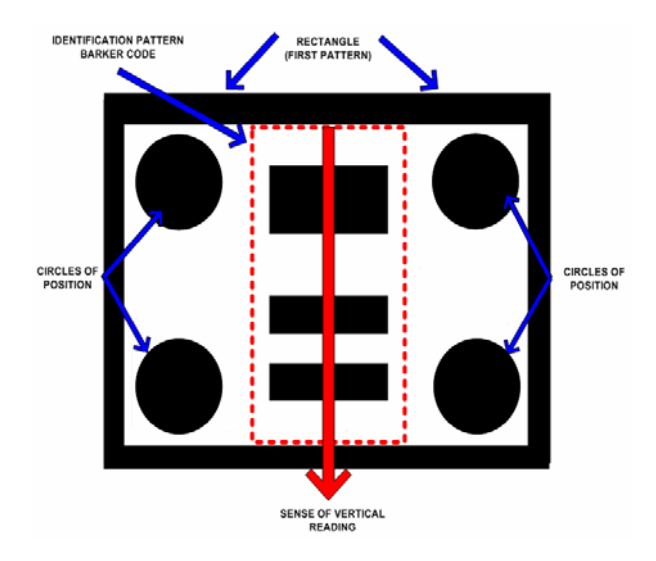


Fig. 1. Characteristics of the Artificial Mark.

obtain the relative position of the AW. The description of these elements is presented in later subsections:

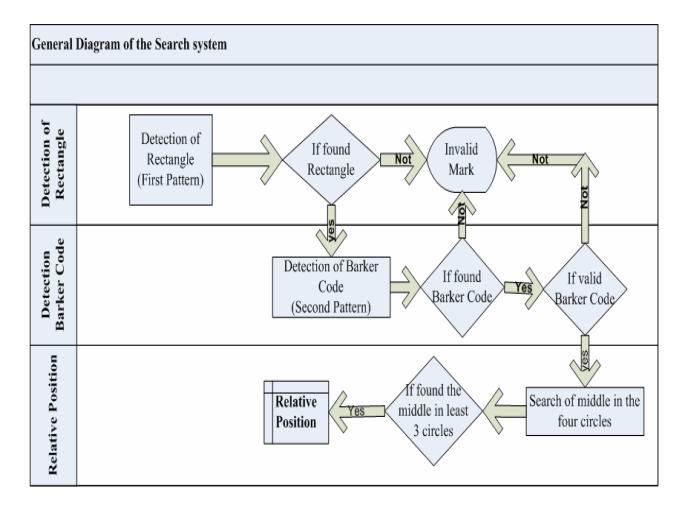


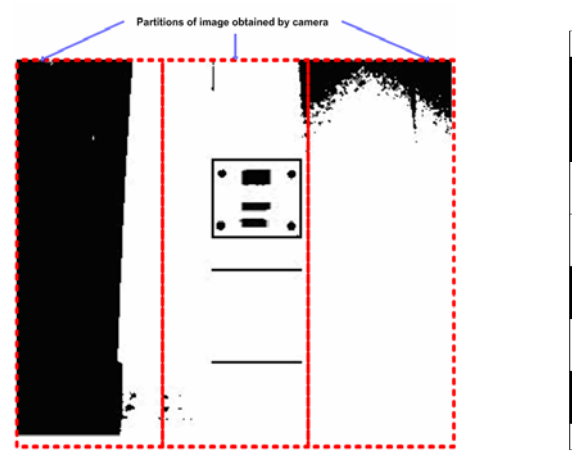
Fig. 2. General Diagram of the Search system.

3.1 Detection of Rectangle

In this stage the Search system scans through the captured image the first evidence (rectangle) that suggests the existence of a valid mark (see figure 3-left). In order to reduce the computational time of processing, the image (in binary scale) is subdivided into three parts for the detection of the rectangle.

3.2 Detection of Barker Code

The Barker code pattern chosen in this process is a Barker code with length of 7 bits. The structure is [1, 1, -1, 1, -1, 1] which fulfills the property of autocorrelation that presents an accused peak when the sequence fits with a pattern. For simplicity, a method of direct codification of the image was adopted. Black stripe=1, white stripe = -1 (see figure 3- right).



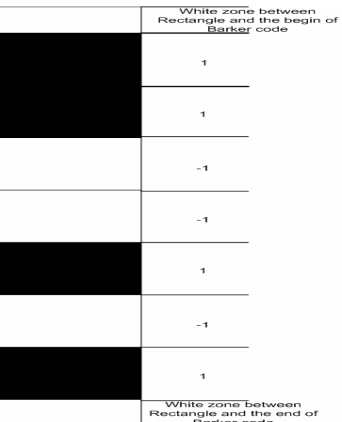


Fig. 3. Left: Captured image from fixed camera. Right: Design of Barker code of 7 bits.

The detection algorithm consists of two main parts, the phase-search and the phase-confirmation.

In the phase-search, the entry of the algorithm is a column (gray levels) from the image to be processed. The scan starts from the initial X-Y coordinates of the found rectangle. Then, an important transition from white to black and vice versa is searched for each pair of columns of the image.

The procedure of search of abrupt changes in the levels of intensity of the image is implemented through a derivative filter of the form:

$$O(k) = I(k+1) - I(k-1)$$
 (1)

Where I(k) is the nth row of entry of the scanned column and O(k) is the nth row of the output image [5].

The output filtered image allows detecting remarkable changes in levels of intensity by localizing characteristic peaks of a Barker code that exceed a threshold given by:

$$O(p) = sg[O(k)] \bullet [(|O(k)| \phi U_p) \& (|O(k)| \ge |O(k-1)|) \& (|O(k)| \le |O(k+1)|)]$$
(2)

Where: $U_P = \sqrt{2 * \frac{1}{n} \sum_{1}^{N} O^2(n)}$

The sign (sg) of peak in the intensity levels allows us to know which transition occurred (- 1 of white to black and 1 of black to white).

Once we have found the significant peaks in the levels of intensity of the image, the following step is to discard all those peaks that do not correspond in number and sequence of the transitions of the Barker code used. For it we used the knowledge of the correct sequence which must be $S(i) = \begin{bmatrix} -1,+1,-1,+1,-1,+1 \end{bmatrix}$ where S(i) represents each possible group with six consecutive peaks.

If in the previous procedure has been detected a set of samples that contain a correct sequence in the transitions of a Barker code, then it is decoded as a possible valid Barker code. Later to reject the existence of a false code, the gray scale image is normalized to correlate it with a synthesized Barker code in the phase-confirmation. The normalized correlation between both elements is defined as:

$$C_n = \frac{\sum (I(x, y) - m_I)(h(x, y) - m_h)/N}{\sigma_I \sigma_h}$$
(3)

Where:

 C_n =Result of normalized correlation.

I(x, y) =Original image.

h(x, y) =Synthesized Barker code pattern.

 $m_1 m_h =$ Image mean value of the original image and code pattern respectively.

 $\sigma_I \sigma_h$ = Variation average of the pixels in relation to the image mean value.

N = Number of overlapped pixels between original image and code pattern.





Fig 4. Left: Barker code detected on the image. Right: Synthesized Barker code.

If the value obtained by the normalized correlation process is C = 1 then exists a perfect correspondence between the image with the barker code detected (See figure 4-left) and the pattern compared (see figure 4-right).

In this experiment, it was considered as valid mark that one that exceeded a threshold of 0.72 in the correlation process. The algorithm used for the search of valid Barker code is based on the algorithms used in previous works [5]. The efficiency of the algorithm consists on carrying out the process of correlation not as a process of search of the barker code, but as a method of confirmation for those possible detected valid codes within the captured image.

3.3 Relative Position

This stage has been split in two main parts. Once that it has been detected and confirmed the existence of a code that indicates the presence of a valid mark, the following step is to find the center of at least three of the four circles placed in the corners of the artificial mark to find the relative position between camera and mark.

3.3.1 Segmentation of Circles and Determination of the Centroid Coordinates

The image is initially divided into two sub windows for the search of the circles: the upper sub window to cover the two high circles and the inferior sub window to cover the two low circles. The search of the circles is conducted using the a priori information (each circle was placed in each one of the corners of the rectangle in the artificial mark). We use this knowledge for saving computation time. For each of the four sub windows, the algorithm compute the vertical and horizontal diameter of each circle of the image using the same method of differentiation (Eq. 1) used in the detection of the Barker code. The scanning algorithm produce the segmented circle as is shown in figure 5. Once done this, the centroid coordinates of the each circle is computed by the following equations:

$$C_{XM} = C_{XYL} + \frac{C_{XYR} - C_{XYL}}{2} \tag{4}$$

$$C_{YM} = C_{XYT} + \frac{C_{XYD} - C_{XYT}}{2} \tag{5}$$

Where:

 C_{XM} = Coordinate on X of circle centroid.

 C_{YM} =Coordinate on Y of circle centroid.

 C_{YYR} =Coordinate on axis XY of border right

 C_{XYI} =Coordinate on axis XY of border left.

 C_{XYT} =Coordinate on axis XY of border top.

 C_{XYT} = coordinate on axis X 1 or border top.

 C_{XYD} =Coordinate on axis XY of border down.

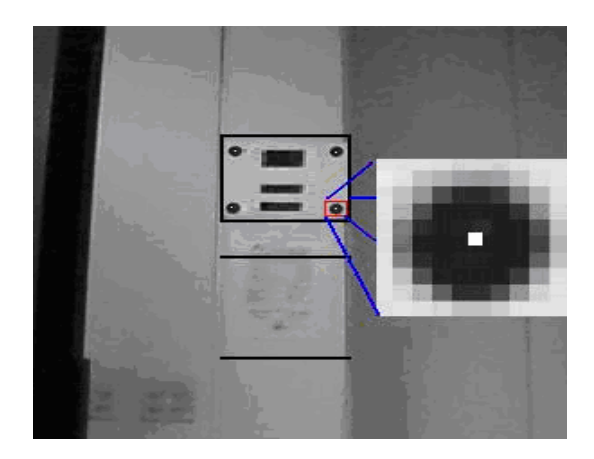


Fig. 5. Detection of circle centroid.

3.3.2 Algorithm for Position Computation

A basic scheme of the algorithm for the recovery of the position is show in the following figure:

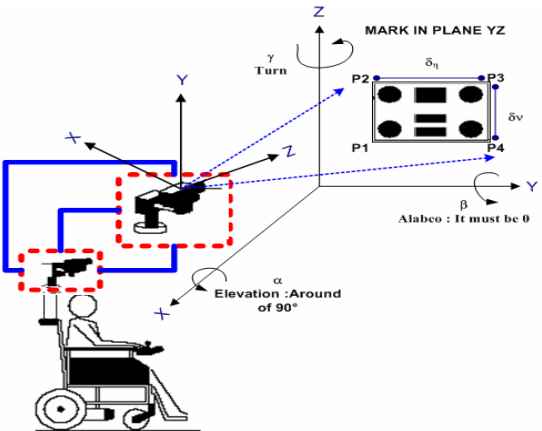


Fig. 6. Basic scheme of algorithm of search of relative position.

This algorithm is based fundamentally on the image shown in figure 6. From this we can recognize two triangular structures formed by two orthogonal oriented vectors referenced by the vector r_1 and r_3 (see figure 7).

In both structures r_1 as r_3 are formed by the following sets of points and oriented segments:

$$r_1 \to [p_1, p_2, p_4, l_{12}, l_{14}]$$
 (6)
 $r_3 \to [p_3, p_2, p_4, l_{32}, l_{34}]$ (7)

$$r_3 \to [p_3, p_2, p_4, l_{32}, l_{34}]$$
 (7)

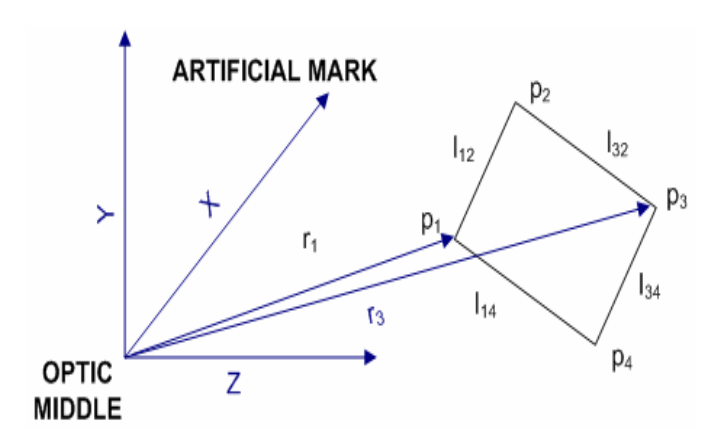


Fig. 7. Recovery of position.

Assuming that α and β it is well-known, and extracting the appropriate subgroup of the transformations of rotation and translation of the camera respect to the artificial mark we obtain [9]:

$$\begin{bmatrix} u_2 - u_1 \\ v_2 - v_1 \end{bmatrix} z_1 = \begin{bmatrix} -\delta_v u_2 \cos(\alpha) \\ \delta_v [\lambda \sin(\alpha) - v_2 \cos(\alpha)] \end{bmatrix}$$

$$\begin{bmatrix} u_4 - u_3 \\ v_4 - v_3 \end{bmatrix} z_3 = \begin{bmatrix} \delta_v u_4 \cos(\alpha) \\ -\delta_v [\lambda \sin(\alpha) - v_4 \cos(\alpha)] \end{bmatrix}$$
(8)

Where u_i and v_i are the coordinates horizontal and vertical of the projection of the centroids of pi on the plane image of the camera. λ is referred by the focal length; δ_v and δ_h are the lengths of the segments horizontal and vertical defined by the points π and α as the elevation angle of the camera.

From the system preview (Eq. 8) are obtained the distances z_1 and z_3 to the points p_1 and p_3 . Known these distances, the determination of the angle of turn is made by means of:

$$\begin{bmatrix} (u_4 - u_1) \frac{z_1}{\delta h} \\ (v_4 - v_1) \frac{z_1}{\delta_h} \\ (u_2 - u_3) \frac{z_3}{\delta_h} \\ (v_2 - v_3) \frac{z_3}{\delta_L} \end{bmatrix} = \begin{bmatrix} \lambda & u_4 \sin(\alpha) \\ 0 & [\lambda \cos(\alpha) + v_4 \sin(\alpha)] \\ -\lambda & -u_2 \sin(\alpha) \\ 0 & -[\lambda \cos(\alpha) + v_2 \sin(\alpha)] \end{bmatrix} \begin{bmatrix} Sin(\gamma) \\ Cos(\gamma) \end{bmatrix}$$

$$(9)$$

With this last equation we obtain the matrix of rotation $R = f(\alpha, \beta, \gamma)$. The recovery of the position-direction of the camera with respect to the position of the artificial mark is to carry out knowing the vectors r_1 and r_3 [5-8].

Results

The efficiency of the system was verified by a series of tests detecting diverse marks placed in strategic places of a room. Once located the rectangle that indicates the presence of a possible artificial mark, the next step was to confirm the validity of the mark, through the fast search algorithm of abrupt changes in the gray levels of image (Barker code). Such as it is indicated in the figure 8, the result shows a correlation factor of 0.98. It ratifies the legitimacy of the code found according to the criteria exposed in the previous sections. It's worth noting that of the number total of made tests were possible to detect and validate 60% of the placed marks.

The figure 9 shows the location of coordinates XY of the rectangle detected (see fig. 4 left) in the image obtained by the camera mounted over the AW in the first stage of system.

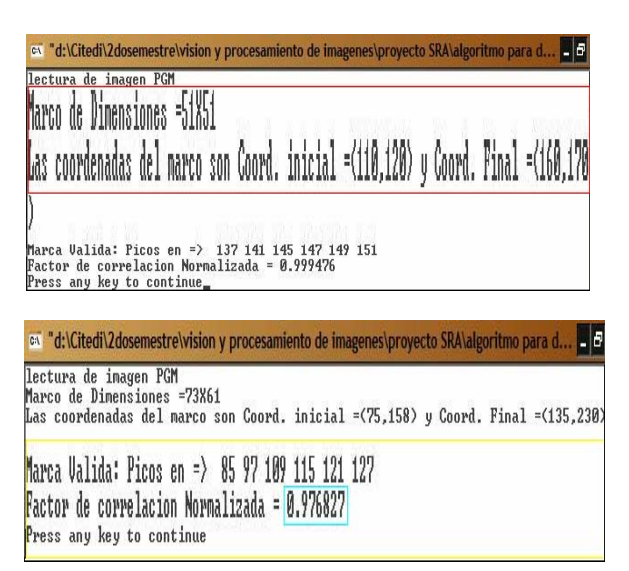


Fig. 8. Detection and validation of the artificial mark.

The figure 9 shows some preliminary experimental results of the localization estimation algorithm of the AW for distances between 0 to 3 m from the artificial mark. This figure shows that the algorithm with four landmark points defined and some previous knowledge about the α and β angles, the estimate position from the camera to landmark presents good results. Finally these experimental results have shown that the artificial landmark is suited for robot localization and n navigation.

Images tests 3 2 0 1 0 1 2 3 X(m) coordinates

Fig. 9. Experimental results of the localization estimation algorithm of the AW.

Acknowledgements. The authors appreciate the support of SIP-IPN, for the support of this research project under grant 20071470 and 20070032.

References

- 1. Bernd Jähne, "Digital Image Processing" New York, Springer Verlag, 1991
- 2. Kenneth R. Castleman, "Digital Image Processing", New Jersey, Prentice Hall, 1996
- Rafael c. Gonzales, Richard E. Woods, "Digital Image Processing", New Jersey, Prentice Hall, 2002
- M. Marron Romera, J. Carlos García, "Sistema de navegación autónoma en entornos interiores estructurados", Available: http://www.depeca.uah.es/personal/marta/TELEC-TFC.pdf
- 5. J. C. García García, M. Manzo, J. Ureña Ureña, M. Marron Romera, "Auto localización y posicionamiento mediante marcas artificiales codificadas", Available: http://www.depeca.uah.es/personal/jcarlos/SRAs/Tesis-pwd-JC-Sistema% 20 Posicionamiento.pdf
- 6. E. Santiso, M. Mazo, J. Ureña, J. A. Jiménez, J. C. Garcia, "Extracción de características para posicionamiento absoluto de robots móviles en interiores", Available: http://www.depeca.uah.es/personal/alvaro/parmei/docs_libres/PARMEI-trps-seguimiento_23Abril.pdf
- V. Castello Martínez, "Localización y descodificación de códigos de barras en imágenes digitales", Available: http://www3.uji.es/~vtraver/e80/E80_Vicente_Castello.pdf
- 8. E. Aguirre, M Gómez, R. Muñoz, C. Ruiz, "Sistema Multi-agente que emplea visión active y ultrasonidos aplicados a navegación con comportamientosdifusos", Available: http://decsai.ugr.es/~salinas/publications/waf2003.pdf
- 9. R. M. Haralick and L. G. Shapiro, Computer and robot vision, vol II. Addison-Wesley Publishing company. 1993